THERMAL PERFORMANCE OF NANOFLUID FILLED SOLAR FLAT PLATE COLLECTOR

Rehena Nasrin* and M. A. Alim

Department of Mathematics, Bangladesh University of Engineering & Technology, Dhaka-1000, Bangladesh.

Email: raity11@gmail.com

ABSTRACT

A numerical study has been conducted to investigate the forced convection through a flat plate solar collector (FPSC). The water Cu nanofluid is used as the working fluid inside the riser pipe of the solar collector. The governing differential equations with boundary conditions are solved by Finite Element Method using Galerkin's weighted residual scheme. The computation domain is discretized by triangular element with six nodes. The effects of major system parameters on the forced convection heat transfer are simulated. These parameters include the the solar irradiation (I) and diameter (D) of the riser pipe. Comprehensive average Nusselt number, mean temperature, mean velocity, percentage of collector efficiency, output temperature for both nanofluid and base fluid through the absorber tube are presented as functions of the pertaining parameters mentioned above. The numerical results show that the highest heat transfer rate is observed for both the highest I and lowest D. Percentage of collector efficiency enhances for growing I and falling D.

Keywords: Thermal performance, Flat plate solar collector, Finite element method, Water-Cu nanofluid, Solar irradiation.

1. INTRODUCTION

The flat-plate solar collector is commonly used today for the collection of low temperature solar thermal energy. It is used for solar water-heating systems in homes and solar space heating. Because of the desirable environmental and safety aspects it is widely believed that solar energy should be utilized instead of other alternative energy forms, even when the costs involved are slightly higher. Solar collectors are key elements in many applications, such as building heating systems, solar drying devices, etc. Solar energy has the greatest potential of all the sources of renewable energy especially when other sources in the country have depleted. The fluids with solid-sized nanoparticles suspended in them are called "nanofluids." Applications of nanoparticles in thermal field are to enhance heat transfer from solar collectors to storage tanks, to improve efficiency of coolants in transformers.

Lund [1] analyzed general thermal behavior of parallel-flow flat-plate solar collector absorbers. Nag et al. [2] analyzed parametric study of parallel flow flat plate solar collector using finite element method. Piao et al. [3] studied forced convective heat transfer in cross-corrugated solar air heaters. Kolb et al. [4] experimentally studied solar air collector with metal matrix absorber. Tripanagnostopoulos et al. [5] investigated solar collectors with colored absorbers. Kazeminejad [6] numerically analyzed two dimensional parallel flow flat-plate solar collectors. Temperature distribution over the absorber plate of a parallel flow flat-plate solar collector was analyzed with one- and two-dimensional steady-state conduction equations with heat generations. Lambert et al. [7] conducted Enhanced heat transfer using oscillatory flows in solar collectors. They proposed the use of oscillatory laminar flows to enhance the transfer of heat from solar collectors. The idea was to explore the possibility of transferring the heat collected from a solar device to a storage tank by means of a zeromean oscillating fluid contained in a tube.

Selected nanofluids might improve the efficiency of direct absorption solar thermal collectors. To determine the effectiveness of nanofluids in solar applications, their ability to convert light energy to thermal energy must be known. That is, their absorption of the solar spectrum must be established. Struckmann [8] analyzed flat-plate solar collector where efforts had been made to combine a number of the most important factors into a single equation and thus formulate a mathematical model which would describe the thermal performance of the collector in a computationally efficient manner. Azad [9] investigated interconnected heat pipe solar collector. Performance of a prototype of the heat pipe solar collector was experimentally examined and the results were compared with those obtained through theoretical analysis. Tyagi et al. [10] investigated Predicted efficiency of a low-temperature nanofluid- based direct absorption solar collector. It was observed that the presence of nanoparticles increased the absorption of incident radiation by more than nine times over that of pure water. According to the results obtained from this study, under

similar operating conditions, the efficiency of a DAC using nanofluid as the working fluid was found to be up to 10% higher than that of a flat-plate collector. Generally a direct absorption solar collector (DASC) using nanofluids as the working fluid performs better than a flat-plate collector. Much better designed flat-plate collectors might be able to match a nanofluid based DASC under certain conditions. Otanicar et al. [11] studied nanofluid-based direct absorption solar collector. They reported on the experimental results on solar collectors based on nanofluids made from a variety of nanoparticles carbon nanotubes, graphite, and silver. They demonstrated efficiency improvements of up to 5% in solar thermal collectors by utilizing nanofluids as the absorption mechanism. In addition the experimental data were compared with a numerical model of a solar collector with direct absorption nanofluids.

Álvarez et al. [12] studied finite element modelling of a solar collector. A mathematical model of a serpentine flat-plate solar collector using finite elements was presented. Karanth et al. [13] performed numerical simulation of a solar flat plate collector using discrete transfer radiation model (DTRM)–a CFD Approach. Dynamics (CFD) by employing conjugate heat transfer showed that the heat transfer simulation due to solar irradiation to the fluid medium, increased with an increase in the mass flow rate. Also it was observed that the absorber plate temperature decreased with increase in the mass flow rate. Martń et al. [14] also analyzed experimental heat transfer research in enhanced flat-plate solar collectors. To test the enhanced solar collector and compare with a standard one, an experimental side-by-side solar collector test bed was designed and constructed. Enhancement of flat-plate solar collector thermal performance with silver nano-fluid was conducted by Polvongsri and Kiatsiriroat [15]. With higher thermal conductivity of the working fluid the solar collector performance could be enhanced compared with that of water. The solar collector efficiency with the nano-fluid was still high even the inlet temperature of the working fluid was increased.

Taylor et al. [16] analyzed nanofluid optical property characterization: towards efficient direct absorption solar collectors. Their study compared model predictions to spectroscopic measurements of extinction coefficients over wavelengths that were important for solar energy (0.25 to 2.5 μm). Modeling of flat-plate solar collector operation in transient states was conducted by Saleh [17]. This study presents a one-dimensional mathematical model for simulating the transient processes which occur in liquid flat-plate solar collectors. The proposed model simulated the complete solar collector system including the flat-plate and the storage tank. Amrutkar et al. [18] studied solar flat plate collector analysis. The objective of their study was to evaluate the performance of FPC with different geometric absorber configuration. It was expected that with the same collector space higher thermal efficiency or higher water temperature could be obtained. Karuppa et al. [19] experimentally investigated a new solar flat plate collector. Experiments had been carried out to test the performance of both the water heaters under water circulation with a small pump and the results were compared. The results showed that the system could reach satisfactory levels of efficiency. Zambolin [20] theoretically and experimentally performed solar thermal collector systems and components. Testing of

thermal efficiency and optimization of these solar thermal collectors were addressed and discussed in this work.

Sandhu [21] experimentally studied temperature field in flat-plate collector and heat transfer enhancement with the use of insert devices. Various new configurations of the conventional insert devices were tested over a wide range of Reynolds number (200-8000). Comparison of these devices showed that in laminar flow regime, wire mesh proved to be an effective insert device and enhanced Nusselt number by 270% while in turbulent flow regime. While in Reynolds number range 2700-8000, concentric coil insert significantly increased the heat transfer and an increase of 460% in Nusselt number was witnessed. Mahian et al. [22] performed a review of the applications of nanofluids in solar energy. The effects of nanofluids on the performance of solar collectors and solar water heaters from the efficiency, economic and environmental considerations viewpoints and the challenges of using nanofluids in solar energy devices were discussed. Natarajan & Sathish [23] studied role of nanofluids in solar water heater. Heat transfer enhancement in solar devices is one of the key issues of energy saving and compact designs. The aim of this paper was to analyze and compare the heat transfer properties of the nanofluids with the conventional fluids. Dara et al. [24] conducted evaluation of a passive flat-plate solar collector. The research investigated the variations of top loss heat transfer coefficient with absorber plate emittance; and air gap spacing between the absorber plate and the cover plate. Iordanou [25] investigated flat-plate solar collectors for water heating with improved heat Transfer for application in climatic conditions of the mediterranean region. The aim of this research project was to improve the thermal performance of passive flat plate solar collectors using a novel cost effective enhanced heat transfer technique. This work focused on the process of energy conversion from the collector to the working fluid. This was accomplished by employing an aluminium grid placed in the channels of a collector to induce a gradient of heat capacitance. The numerical simulations focused on the thermal and hydrodynamic behavior of the collector.

Conduction convection radiation processes of a solar collector using FEA was performed by Moningi [26]. Radiation dominated the other two processes. It being non-linear phenomena required an iterative procedure to solve problems analytically, which was quite difficult. So, he tried to find the temperature distribution of the solar collector using FEA. Chabane et al. [27] studied thermal performance optimization of a flat plate solar air heater. Experimentally investigates of single pass solar air heater without fins; present the aims to review of designed and analyzed a thermal efficiency of flat-plate solar air heaters. The received energy and useful energy rates of the solar air heaters were evaluated for various air flow rates were (0.0108, 0.0145, 0.0161, 0.0184 and 0.0203 kg.s⁻¹) are investigated. Optimum values of air mass flow rates were suggested maximizing the performance of the solar collector. Nasrin and Alim [28-29] studied Soret and Dufour effects on double diffusive natural convection using nanofluid with different nanoparticles-filled solar collector.

In the light of above discussions, it is seen that there has been a good number of works in the field of heat transfer system through a flat plate solar collector. In spite of that there is some scope to work with fluid flow, cooling system and enhancement of collector efficiency using nanofluid.

In this paper, the thermal performance of a flat plate solar collector is studied numerically. The objective of this paper is to present heat transfer system through a solar collector for the effect of solar irradiation and diameter of the riser pipe.

2. MATHEMATICAL MODELING

If I is the intensity of solar radiation, incident on the aperture plane of the solar collector having a collector surface area of A, then the amount of solar radiation received by the collector is

$$Q_i = I.A \tag{1}$$

However, a part of this radiation is reflected back to the sky, another component is absorbed by the glazing and the rest is transmitted through the glazing and reaches the absorber plate as short wave radiation. Therefore the conversion factor indicates the percentage of the solar rays penetrating the transparent cover of the collector (transmission) and the percentage being absorbed. Basically, it is the product of the rate of transmission of the cover (λ) and the absorption rate of the absorber (κ).

Thus

$$Q_{recv} = I(\lambda\kappa)A \tag{2}$$

As the collector absorbs heat its temperature is getting higher than that of the surrounding and heat is lost to the atmosphere by convection and radiation. The rate of heat loss (Q_{loss}) depends on the collector overall heat transfer coefficient (h) and the collector temperature

$$Q_{loss} = hA(T_{col} - T_{amb}) \tag{3}$$

Thus, the rate of useful energy extracted by the collector (Q_{usfl}), expressed as a rate of extraction under steady state conditions, is proportional to the rate of useful energy absorbed by the collector, less the amount lost by the collector to its surroundings. This is expressed as

$$Q_{usfl} = Q_{recv} - Q_{loss} = I(\lambda\kappa)A - hA(T_{col} - T_{amb}) \tag{4}$$

where T_{col} and T_{amb} are collector temperature and ambient temperature outside the collector respectively.

It is also known that the rate of extraction of heat from the collector may be measured by means of the amount of heat carried away in the fluid passed through it, which is

$$Q_{usfl} = mC_p(T_{out} - T_{in}) \tag{5}$$

Equation (4) may be inconvenient because of the difficulty in defining the collector average temperature. It is convenient to define a quantity that relates the actual useful energy gain of a collector to the useful gain if the whole collector surface were at the fluid input temperature. This quantity is known as "the collector heat removal factor (F_R)" and is expressed as:

$$F_R = \frac{mC_p(T_{out} - T_{in})}{A[I(\lambda\kappa) - h(T_{in} - T_{amb})]} \tag{6}$$

where T_{in} and T_{out} are inlet and outlet mean temperature of fluid, respectively.

The maximum possible useful energy gain in a solar collector occurs when the whole collector is at the inlet fluid temperature. The actual useful energy gain (Q_{usfl}), is found by multiplying the collector heat removal factor (F_R) by the maximum possible useful energy gain. This allows the rewriting of equation (4):

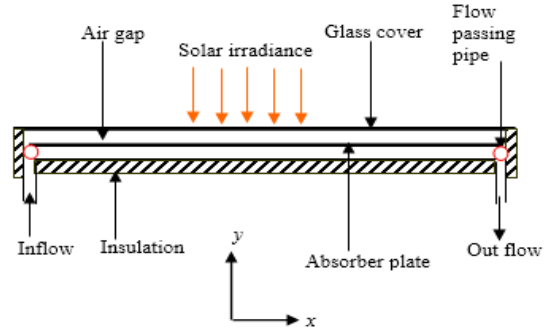$$Q_{usfl} = F_R A[I(\lambda\kappa) - h(T_{in} - T_{amb})] \tag{7}$$

Figure 1. Schematic diagram of the solar collector

Equation (7) is a widely used relationship for measuring collector energy gain and is generally known as the "Hottel-Whillier-Bliss equation". The heat flux per unit area q is now denoted as

$$\frac{Q_{usfl}}{A} = q = I\lambda\kappa - h(T_{in} - T_{amb}) \tag{8}$$

A cross section of the system considered in the present study is shown in Fig. 1. The system consists of a flat plate solar collector. The numerical computation is carried on taking single riser pipe of FPSC. The glass cover is at the top of the FPSC. It is highly transparent and anti-reflected (called the glazing). The glass top surface is exposed to solar irradiation. It is made up of borosilicate which has thermal conductivity of 1.14 W/mK and refractive index of 1.47, specific heat of 750 J/kgK and coefficient of sunlight transmission of 95%. The wavelength of visible light is roughly 700 nm. Thickness of glass cover is 0.005m. There is an air gap of 0.005m between glass cover and absorber plate. Air density = 1.269 Kg/m³, specific heat = 287.058 J/kgK and thermal conductivity = 0.0243 W/mK. All these properties of air domain represent air of temperature at 298K. A dark colored copper absorber plate is under the air gap. Length, width and thickness of the absorber plate are 1m, 0.15m and 0.0005m respectively. Coefficients of heat absorption and emmision of copper absorber plate are 95% and 5% respectively. The riser pipe has inner diameter 0.01 m and thickness 0.0005m. The riser tube is also made in copper metal.

The working fluid in the collector is water-based nanofluid containing Cu nanoparticles. The nanoparticles are generally spherical shaped and diameter is taken as 5 nm. The nanofluid is considered as single phase flow and surfactant analysis is neglected. A, L and D are the surface area of the collector, length and diameter of the riser. In the present problem, it can be considered that the flow is considered to be laminar and there is no viscous dissipation. The nanofluid

is assumed incompressible. It is taken that water and nanoparticles are in thermal equilibrium and no slip occurs between them. The density of the nanofluid is approximated by the Boussinesq model. Only steady state case is considered.

The computation domain is a fluid passing copper riser pipe which is attached ultrasonically to the absorber plate. The fluid enters from the left inlet and getting heat form solid boundaries and finally exits from the right inlet of the riser pipe of a flat plate solar collector. The incident radiation is considered to be the incoming solar radiation. For the study of the principal behavior of the nanofluid based FPSC, atmospheric absorption is neglected in this calculation. Once the intensity distributions are evaluated, the energy balance on the solar collector is performed and the temperature profile within it is obtained. In order to carry out these steps, some assumptions are made.

$$\frac{\partial u}{\partial x} + \frac{\partial v}{\partial y} = 0 \tag{9}$$

$$\rho_{nf}\left(u\frac{\partial u}{\partial x} + v\frac{\partial u}{\partial y}\right) = -\frac{\partial p}{\partial x} + \mu_{nf}\left(\frac{\partial^2 u}{\partial x^2} + \frac{\partial^2 u}{\partial y^2}\right) \tag{10}$$

$$\rho_{nf}\left(u\frac{\partial v}{\partial x} + v\frac{\partial v}{\partial y}\right) = -\frac{\partial p}{\partial y} + \mu_{nf}\left(\frac{\partial^2 v}{\partial x^2} + \frac{\partial^2 v}{\partial y^2}\right) \tag{11}$$

$$u\frac{\partial T}{\partial x} + v\frac{\partial T}{\partial y} = \alpha_{nf}\left(\frac{\partial^2 T}{\partial x^2} + \frac{\partial^2 T}{\partial y^2}\right) \tag{12}$$

$$\left(\frac{\partial^2 T_a}{\partial x^2} + \frac{\partial^2 T_a}{\partial y^2}\right) = 0 \tag{13}$$

The thermal diffusivity $\alpha_{nf} = k_{nf}\big/\left(\rho C_p\right)_{nf}$

The density $\rho_{nf} = \left(1-\phi\right)\rho_f + \phi\rho_s$

The heat capacitance $\left(\rho C_p\right)_{nf} = \left(1-\phi\right)\left(\rho C_p\right)_f + \phi\left(\rho C_p\right)_s$

The viscosity of the nanofluid is considered by the Pak and Cho correlation [30]. This correlation is given as $\mu_{nf} = \mu_f\left(1+39.11\phi + 533.9\phi^2\right)$

The thermal conductivity of Maxwell Garnett (MG) model [31] is $k_{nf} = k_f\dfrac{k_s + 2k_f - 2\phi\left(k_f - k_s\right)}{k_s + 2k_f + \phi\left(k_f - k_s\right)}$

The boundary conditions are:
at all solid boundaries: $u = v = 0$

at the solid-fluid interface: $k_{nf}\left(\dfrac{\partial T}{\partial y}\right)_{nf} = k_{solid}\left(\dfrac{\partial T_a}{\partial y}\right)_{solid}$

at the inlet boundary: $T = T_{in}$, $u = u_{in}$

at the outlet boundary: convective boundary condition $p = 0$

at the top surface of absorber: heat flux

$-k_a\dfrac{\partial T_a}{\partial y} = q = I\tau\kappa - h\left(T_{in} - T_{amb}\right)$

at outer surface of riser pipe: $\dfrac{\partial T}{\partial y} = 0$

The above equations are non-dimensionalized by using the following dimensionless dependent and independent variables:

$$X = \frac{x}{L}, Y = \frac{y}{L}, U = \frac{u}{U_{in}}, V = \frac{v}{U_{in}},$$

$$P = \frac{p}{\rho_f U_{in}^{\,2}}, \theta = \frac{\left(T - T_{in}\right)k_f}{qL}, \theta_a = \frac{\left(T_a - T_{in}\right)k_a}{qL}$$

Then the non-dimensional governing equations are

$$\frac{\partial U}{\partial X} + \frac{\partial V}{\partial Y} = 0 \tag{14}$$

$$U\frac{\partial U}{\partial X} + V\frac{\partial U}{\partial Y} = -\frac{\rho_f}{\rho_{nf}}\frac{\partial P}{\partial X} + \frac{v_{nf}}{v_f}\frac{1}{Re}\left(\frac{\partial^2 U}{\partial X^2} + \frac{\partial^2 U}{\partial Y^2}\right) \tag{15}$$

$$U\frac{\partial V}{\partial X} + V\frac{\partial V}{\partial Y} = -\frac{\rho_f}{\rho_{nf}}\frac{\partial P}{\partial Y} + \frac{v_{nf}}{v_f}\frac{1}{Re}\left(\frac{\partial^2 V}{\partial X^2} + \frac{\partial^2 V}{\partial Y^2}\right) \tag{16}$$

$$U\frac{\partial \theta}{\partial X} + V\frac{\partial \theta}{\partial Y} = \frac{1}{RePr}\frac{\alpha_{nf}}{\alpha_f}\left(\frac{\partial^2 \theta}{\partial X^2} + \frac{\partial^2 \theta}{\partial Y^2}\right) \tag{17}$$

$$\left(\frac{\partial^2 \theta_a}{\partial X^2} + \frac{\partial^2 \theta_a}{\partial Y^2}\right) = 0 \tag{18}$$

where $Pr = \dfrac{v_f}{\alpha_f}$ is the Prandtl number, $Re = \dfrac{U_{in}L}{v_f}$ is the Reynolds number.

The corresponding boundary conditions take the following form:
at all solid boundaries: $U = V = 0$

at the solid-fluid interface: $k_{nf}\left(\dfrac{\partial \theta}{\partial Y}\right)_{nf} = k_{solid}\left(\dfrac{\partial \theta_a}{\partial Y}\right)_{solid}$

at the inlet boundary: $\theta = 0$, $U = 1$
at the outlet boundary: convective boundary condition $P = 0$

at the top surface of absorber: heat flux $\dfrac{\partial \theta_a}{\partial Y} = -\dfrac{k_f}{k_{nf}}$

at outer surface of riser pipe: $\dfrac{\partial T}{\partial y} = 0$

The non-dimensional form of local convective heat transfer at the top surface is $\overline{Nu} = -\dfrac{k_{nf}}{k_f}\dfrac{\partial \theta}{\partial Y}$.

By integrating the local Nusselt number over the top heated surface, the average convective heat transfer along the heated wall of the collector is used by Saleh et al. [32] as $Nu = \displaystyle\int_0^1 \overline{Nu}\, dX$.

The mean bulk temperature and average sub domain velocity of the fluid inside the collector may be written as $\theta_{av} = \int \theta\, d\overline{V}/\overline{V}$ and $V_{av} = \int V\, d\overline{V}/\overline{V}$, where $\overline{V}$ is the volume of the collector.

A measure of a flat plate collector performance is the collector efficiency (η) defined as the ratio of the useful energy gain (Q_{usfl}) to the incident solar energy. The instantaneous thermal efficiency of the collector is:

$$\eta = \frac{Q_{usfl}}{AI} = \frac{F_R A \left[I(\lambda\kappa) - h(T_{in} - T_{amb}) \right]}{AI}$$

$$= F_R(\lambda\kappa) - F_R h \frac{(T_{in} - T_{amb})}{I}$$

where m is the mass flow rate of the fluid flowing through the collector; C_p is the specific heat at constant pressure.

3. NUMERICAL TECHNIQUE

The Galerkin finite element method Taylor and Hood [33] and Dechaumphai [34] is used to solve the non-dimensional governing equations along with boundary conditions for the considered problem. The equation of continuity has been used as a constraint due to mass conservation and this restriction may be used to find the pressure distribution. The finite element method of Reddy [35] is used to solve the Eqs. (19) - (22), where the pressure P is eliminated by a constraint. The continuity equation (19) is automatically fulfilled for large values of this constraint. Then the velocity components (U, V) and temperature (θ) are expanded using a basis set. The Galerkin finite element technique yields the subsequent nonlinear residual equations. Three points Gaussian quadrature is used to evaluate the integrals in these equations. The non-linear residual equations are solved using Newton–Raphson method to determine the coefficients of the expansions. The convergence of solutions is assumed when the relative error for each variable between consecutive iterations is recorded below the convergence criterion such that $\left| \psi^{n+1} - \psi^n \right| \leq 10^{-4}$, where n is the number of iteration and Ψ is a function of U, V and θ.

3.1 Mesh Generation

In the finite element method, the mesh generation is the technique to subdivide a domain into a set of sub-domains, called finite elements, control volume, etc. The discrete locations are defined by the numerical grid, at which the variables are to be calculated. It is basically a discrete representation of the geometric domain on which the problem is to be solved. The computational domains with irregular geometries by a collection of finite elements make the method a valuable practical tool for the solution of boundary value problems arising in various fields of engineering. Fig. 2 displays the finite element mesh of the present physical domain.
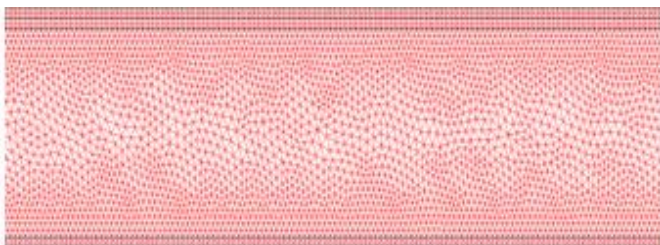

Figure 2. Mesh generation of the FPSC

3.2. Thermo-physical properties

The thermo-physical properties of the nanofluid are taken from Ogut [22] and given in Table 1.

Table 1. Thermo-physical properties of fluid and nanoparticles

Physical Properties	Fluid phase (Water)	Cu
C_p(J/kgK)	4179	385
ρ (kg/m³)	997	8933
k (W/mK)	0.613	400
$\alpha \times 10^7$ (m²/s)	1.47	1163.1

3.3 Grid Independent Test

An extensive mesh testing procedure is conducted to guarantee a grid-independent solution for $Pr = 5.8$, $\phi = 2\%$, $I = 215$W/m² and $Re = 480$ through a riser pipe of a FPSC. In the present work, four different non-uniform grid systems are examined with the number of elements within the resolution field: 42,010, 99,832, 1,50,472,1,68,040 and 1,92,548. The numerical scheme is carried out for highly precise key in the average Nusselt number for water-copper nanofluid ($\phi = 2\%$) as well as base fluid ($\phi = 0\%$) for the aforesaid elements to develop an understanding of the grid fineness as shown in Table 2. From the fourth and fifth column in the Table 2 it is observed that there is no significant change in the rate of heat transfer but time consuming. So considering the non-uniform grid system of 1,68,040 elements is preferred for the computation. This element size is taken from extra fine meshing.

Table 2. Grid test at $Pr = 5.8$, $\phi = 2\%$, $D = 0.01$m, $I = 215$W/m² and $Re = 480$

Elements	42,010	99,832	1,40,472	1,68,040	1,92,548
Nu (Nanofluid)	1.87872	1.99127	2.10934	2.14351	2.14378
Nu (Base fluid)	1.59326	1.69225	1.81524	1.84333	1.84341
Time (s)	127.52	308.75	581.11	897.23	1295.31

4. RESULTS AND DISCUSSIONS

In this section, numerical results of the average Nusselt number, mean bulk temperature, mean sub domain velocity, percentage of collector efficiency and dimensional outlet temperature of the water-copper nanofluid as well as clear water in a flat plate solar collector are shown graphically for various values of solar irradiation (I) and dimensionless inner diameter (D). The considered values of I and D are I = (200 W/m², 215 W/m², 230 W/m² and 250 W/m²), D (= 0.01m, 0.012m, 0.013m and 0.015m) while the solid volume fraction of Cu nanoparticle is $\phi = 2\%$. Here, Reynolds number (Re), Prandtl number (Pr), collector area (A), mass flow rate per unit area (m) are considered as 480, 5.8, 1.8m² and 0.0248Kg/s respectively.

4.1 Heat Transfer rate

The *Nu-I* and *Nu-D* profiles for Cu/water nanofluid as well as base fluid are depicted in Fig. 4(i)-(ii). It is seen from Fig. 3(i) that the average Nusselt number increases with rising solar irradiation for both type fluids. The rate of heat transfer enhances 13% and 9% using 2% concentrated water-copper nanofluid and water respectively for rising solar irradiation (*I*) from 200 W/m² to 250 W/m² when *D* = 0.01m.

Fig. 3(ii) shows that *Nu* devalues slowly with growing inner diameter (*D*) of the riser pipe of a flat plate solar collector. The rate of heat loss for water-Cu nanofluid (ϕ = 2%) is found to be lower than the clear water (ϕ = 0%) due to higher thermal conductivity of solid nanoparticles. Heat loss rate diminishes by 10% and 15% for nanofluid and base fluid respectively at the solar irradiance *I* = 215W/m².
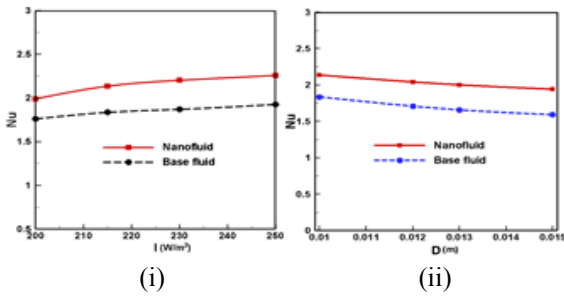

(i)   (ii)

Figure 3. Mean Nusselt number for the effect of (i) *I* at *D* = 0.01m and (i) *D* at *I* = 215 w/m²

4.2 Mean bulk temperature

Fig. 4(i)-(ii) displays mean temperature (θ_{av}) along with the solar radiance and dimensionless inner diameter for both type of fluids. θ_{av} rises sequentially for growing *I* and falling *D*. It is well known that higher values of solar irradiation (*I*) indicate higher temperature of fluids. Due to escalating values of *I* top and bottom surfaces of the riser pipe become more heated. As a result fluids can take more heat from hot walls and become hotter. Here base fluid has lower mean temperature than the water-Cu nanofluid.
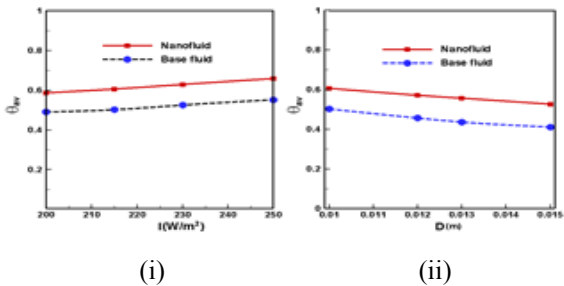

(i)   (ii)

Figure 4. Average temperature for the effect of (i) *I* at *D* = 0.01m and (i) *D* at *I* = 215 w/m²

4.3 Magnitude of average velocity

Magnitude of average velocity vector (V$_{av}$) for the effect of solar irradiation and inner diameter are expressed in the Fig. 5(i)-(ii). V$_{av}$ has notable changes with different values of solar radiance as well as inner diameter of riser pipe. Clear water moves freely than solid concentrated nanofluid.

Growing solar radiance and falling inner diameter enhance the mean velocity of the fluids through the riser pipe of a flat plate solar collector.
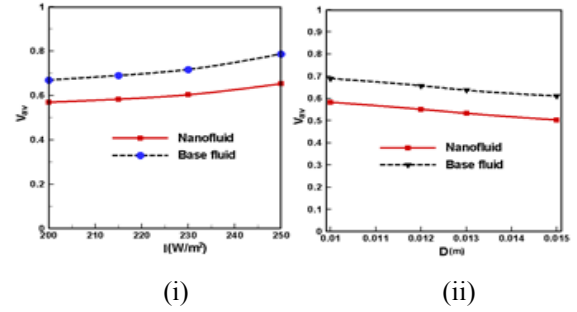

(i)   (ii)

Figure 5. Mean velocity for the effect of (i) *I* at *D* = 0.01m and (i) *D* at *I* = 215 w/m²
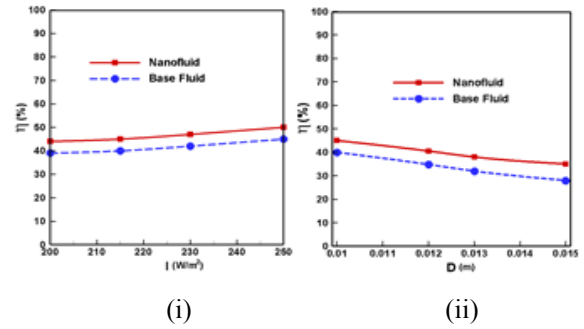

(i)   (ii)

Figure 6. Collector efficiency for the effect of (i) *I* at *D* = 0.01m and (i) *D* at *I* = 215 w/m²

4.4 Collector efficiency

The collector efficiency (η) is plotted against the solar irradiation and inner diameter in Fig. 6(i)-(ii). It is observed from Fig. 6(i) that by introducing greater solar irradiation the collector efficiency increases. More solar irradiance is able to augment heat transfer system through the riser pipe of a flat plate solar collector. In this scheme water/copper nanofluid (ϕ = 2%) performs better than clear water (ϕ = 0%). Thermal efficiency enhances from 44%-50% for nanofluid and 39%-45% for water.

The Fig. 6(ii) shows that the use of small inner diameter of the riser pipe can improve the efficiency of a flat plate solar collector. When the non-dimensional inner diameter increases, the thermal efficiency (η) of the flat plate solar collector diminishes moderately. In other words, the heat extracted from riser pipe by the fluids cannot be increased by growing *D*. Thermal efficiency devalues from 45%-35% for nanofluid and 40%-28% for water.

4.5 Outlet temperature

Fig. 7(i)-(ii) displays the dimensional temperature (K) of water-Cu nanofluid at the middle height of the riser pipe with the influences of solar irradiation and dimensionless inner diameter of the riser pipe. From the figure 7(i) it is observed that the mean output temperature of fluids increases for the increasing values of *I*. The output temperature of nanofluid becomes 312K, 313K, 315K, 317K for nanofluid and 309K, 310K, 311K, 313K for base fluid for *I* = 200W/m², 215 W/m², 230 W/m² and 250 W/m² respectively.

Similarly outlet temperature of Cu/water nanofluid decreases with growing inner diameter (*D*) of the riser pipe.

The output temperature of nanofluid becomes 313K, 312K, 312K and 310K for nanofluid and 310K, 309K, 308K and 307K for base fluid D = 0.01m, 0.012m, 0.013m and 0.15m respectively.
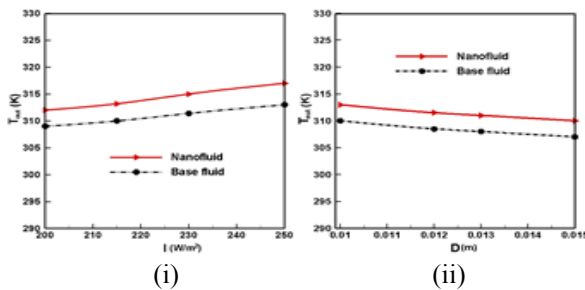

Figure 7. Outlet temperature for the effect of (i) I at D = 0.01m and (i) D at I = 215 w/m^2

5. CONCLUSION

The results of the numerical analysis lead to the following conclusions:
(1) The Cu nanoparticles with the highest I and lowest D are established to be most effective in enhancing performance of heat transfer rate than base fluid.
(2) Average velocity field increases due to growing I and diminishing D.
(3) Collector efficiency is obtained higher for rising I and falling D.
(4) Mean temperature devalues for both fluids with lessening solar radiance and rising inner diameter.

ACKNOWLEDGEMENT

REFERENCES

1. K.O. Lund, General thermal analysis of parallel-flow flat-plate solar collector absorbers, *Solar Energy*, vol. 5, 443, 1986.
2. A. Nag, D. Misra, K.E. De, A. Bhattacharya, S.K. Saha, Parametric study of parallel flow flat plate solar collector using finite element method, In: Num. Methods in Therm. Problems, Proc. of the 6th Int. Conf., Swansea, UK, 1989.
3. Y. Piao, EG. Hauptmann, M. Iqbal, Forced convective heat transfer in cross-corrugated solar air heaters, *ASME Journal of Solar Energy Engg.*, Vol. 116, pp. 212-214, 1994.
4. A. Kolb, ERF Winter, R. Viskanta, Experimental studies on a solar air collector with metal matrix absorber, *Solar Energy*, vol. 65, No. 2, pp. 91–98, 1999.
5. Y. Tripanagnostopoulos, M. Souliotis, T. Nousia, Solar collectors with colored absorbers, *Solar Energy*, vol. 68, pp. 343–356, 2000.
6. H. Kazeminejad, Numerical analysis of two dimensional parallel flow flat-plate solar collector, *Renew. Energy*, vol. 26, pp. 309–323, 2002.
7. A.A. Lambert, S. Cuevas, J.A. del Rı´o, Enhanced heat transfer using oscillatory flows in solar collectors, *Solar Energy*, vol. 80, pp. 1296–1302, 2006.
8. F. Struckmann, Analysis of a Flat-plate Solar Collector, Project Report 2008 MVK160 Heat and Mass Transport, Lund, Sweden, 2008.
9. E. Azad, Interconnected heat pipe solar collector, *IJE Transactions A: Basics*, vol. 22, No. 3, pp. 233, September 2009.
10. H. Tyagi, P. Phelan, R. Prasher, Predicted Efficiency of a Low-Temperature Nanofluid- Based Direct Absorption Solar Collector, *J. of Solar Energy Engg.*, vol. 131/041004-1, 2009.
11. T.P. Otanicar, P.E. Phelan, R.S. Prasher, G. Rosengarten, and R.A. Taylor, Nanofluid-based direct absorption solar collector, *J. of Renew. and Sust. Energy*, vol. 2, pp. 033102, 2010.
12. A. Álvarez, M.C. Muñiz, L.M. Varela, O. Cabeza, Finite element modelling of a solar collector, Int. Conf. on Renew. Energies and Power Quality, Granada (Spain), 2010.
13. K.V. Karanth, M.S. Manjunath, N.Y. Sharma, Numerical simulation of a solar flat plate collector using discrete transfer radiation model (DTRM)–a CFD approach, Proc. of the World Congress on Engg., vol III, WCE 2011, London, U.K.
14. R.H. Martín, A.G. Pinar, J.P. García, Experimental heat transfer research in enhanced flat-plate solar collectors, Solar Thermal Applications, World Renew. *Energy Congress-2011*, pp. 3844-3851.
15. S. Polvongsri and T. Kiatsiriroat, Enhancement of Flat-Plate Solar Collector Thermal Performance with Silver Nano-fluid, The 2nd TSME Int. Conf. on Mech. Engg., Krabi, 2011.
16. R.A. Taylor, P.E. Phelan, T.P. Otanicar, R. Adrian, R. Prasher, Nanofluid optical property characterization: towards efficient direct absorption solar collectors, *Nanoscale Research Letters*, vol. 6, pp. 225, 2011.
17. A.M. Saleh, Modeling of flat-plate solar collector operation in transient states, thesis of Master of Sci. in Engg., 2012, Purdue University, Fort Wayne, Indiana.
18. S.K. Amrutkar, S. Ghodke, Dr.K.N. Patil, Solar flat plate collector analysis, *IOSR J. of Engg*, vol. 2, No. 2, pp.207-213, 2012.
19. R.R.T.K., P. Pavan and D.R. Rajeev, Experimental investigation of a new solar flat plate collector, *Research J. of Engg. Sciences*, vol. 1, No. 4, pp.1-8, 2012.
20. E. Zambolin, Theoretical and experimental study of solar thermal collector systems and components, Scuola di Dottorato di Ricerca in Ingegneria Industriale, Indirizzo Fisica Tecnica.
21. G. Sandhu, Experimental study of temperature field in flat-plate collector and heat transfer enhancement with the use of insert devices, M. of Engg. Sci. thesis, The School of Graduate and Postdoctoral Studies, The University of Western Ontario London, Ontario, Canada, 2013.
22. O. Mahian, A. Kianifar, S.A. Kalogirou, I. Pop, S. Wongwises, A review of the applications of nanofluids in solar energy, *Int. J. of Heat and Mass Trans.*, vol. 57, pp. 582–594, 2013.

23. E. Natarajan & R. Sathish, Role of nanofluids in solar water heater, *Int J Adv Manuf .Technol.* DOI 10.1007/s00170-008-1876-8.

24. J.E Dara, K.O. Ikebudu, N.O. Ubani, C.E. Chinwuko, O.A. Ubachukwu, Evaluation of a passive flat-plate solar collector, *Int. J. of Advancements in Res. & Tech.*, vol. 2, No. 1, 2013.

25. G. Iordanou, Flat-plate solar collectors for water heating with improved heat transfer for application in climatic conditions of the mediterranean region, Doctoral thesis, Durham University.

26. M.K. Moningi, Conduction convection radiation processes of a solar collector using FEA, University of Massachusetts, Amherst.

27. F. Chabane, N. Moummi, S. Benramache, D. Bensahal, O. Belahssen, F.Z. Lemmadi, Thermal performance optimization of a flat plate solar air heater, *Int. J. of Energy & Tech.*, vol. 5, no. 8, pp. 1–6, 2013.

28. R. Nasrin and M.A. Alim, Soret and Dufour effects on double diffusive natural convection in a chamber using nanofluid, *Int. J. of Heat & Tech.*, vol. 30, no. 1, pp. 111-120, 2012.

29. R. Nasrin and M.A. Alim, Dufour-Soret effects on buoyant convection through a nanofluid with different nanoparticles-filled solar collector, *Int. J. of Heat &Tech.*, vol. 31, no. 1, pp. 31-40, 2013.

30. B.C. Pak, Y. Cho, Hydrodynamic and heat transfer study of dispersed fluids with submicron metallic oxide particle, Experimental Heat Transfer, vol. 11, pp. 151-170, 1998.

31. J.C. Maxwell-Garnett, Colours in metal glasses and in metallic films, Philos. *Trans. Roy. Soc. A,* vol. 203, pp. 385–420, 1904.

32. H. Saleh, R. Roslan, I. Hashim, Natural convection heat transfer in a nanofluid-filled trapezoidal enclosure, *Int. J. of Heat and Mass Trans.*, vol. 54, pp. 194–201, 2011.

33. C. Taylor, P. Hood, A numerical solution of the Navier-Stokes equations using finite element technique, *Computer and Fluids*, vol. 1, pp. 73–89, 1973.

34. P. Dechaumphai, Finite Element Method in Engineering, 2nd ed., Chulalongkorn University Press, Bangkok, 1999.

35. J.N. Reddy and D.K. Gartling, The Finite Element Method in Heat Transfer and Fluid Dynamics, CRC Press, Inc., Boca Raton, Florida, 1994.

36. E.B. Ogut, Natural convection of water-based nanofluids in an inclined enclosure with a heat source, *Int. J. of Thermal Sciences*, vol. 48, No. 11, pp. 2063-2073, 2011.

37. S.A. Kalogirou, Solar thermal collectors and applications, *Progress in Energy and Combustion Science*, vol. 30, pp. 231–295, 2004.

NOMENCLATURES

A	Surface area of the collector (m^2)
C_p	Specific heat at constant pressure (J kg^{-1} K^{-1})
d	Inner diameter of riser pipe (m)
D	Dimensionless inner diameter of pipe
h	Local heat transfer coefficient (W m^{-2} K^{-1})
I	Intensity of solar radiation (W m^{-2})
k	Thermal conductivity (W m^{-1} K^{-1})
L	Length of the riser pipe (m)
m	mass flow rate (Kg s^{-1})
Nu	Nusselt number, $Nu = hL/k_f$
Pr	Prandtl number
Re	Reynolds number
T	Dimensional temperature (K)
T_{in}	Input temperature of fluid (K)
T_{out}	Output temperature of fluid (K)
u, v	Dimensional x and y components of velocity (m s^{-1})
U, V	Dimensionless velocities
U_i	Input velocity of fluid (m s^{-1})
X, Y	Dimensionless coordinates
x, y	Dimensional co-ordinates (m)

Greek Symbols

α	Fluid thermal diffusivity (m^2 s^{-1})
ϕ	Nanoparticles volume fraction
v	Kinematic viscosity (m^2 s^{-1})
η	collector efficiency,
θ	Dimensionless temperature
ρ	Density (kg m^{-3})
μ	Dynamic viscosity (N s m^{-2})
V	Dimensionless velocity field

Subscripts

av	average
col	collector
f	fluid
nf	nanofluid
s	solid particle